CHEMISTRY
A EUROPEAN JOURNAL

DOI: 10.1002/chem.200902919

A Triphenylphosphonium-Functionalised Cyclometalated Platinum(II) Complex as a Nucleolus-Specific Two-Photon Molecular Dye

Chi-Kin Koo,[a] Leo K.-Y. So,[a] Ka-Leung Wong,[a] Yu-Man Ho,[a] Yun-Wah Lam,*[a] Michael H.-W. Lam,*[a] Kwok-Wai Cheah,[b] Chopen Chan-Wut Cheng,[c] and Wai-Ming Kwok[c]

Abstract: An organometallic cyclometalated platinum(II) complex, $[Pt(L^3)Cl][PF_6]$, has been synthesised from a specially designed cyclometalating ligand, HL^3 (triphenyl{5-[3-(6-phenylpyridin-2-yl)-1*H*-pyrazol-1-yl]pentyl}phosphonium chloride), that contains a pendant carbon chain carrying a terminal cationic triphenylphosphonium moiety. Aside from its room temperature single-photon luminescent properties in solution, $[Pt(L^3)Cl]^+$ can also produce two-photon-induced luminescence at room temperature upon excitation at 700 nm from a mode-locked Ti:sapphire laser. Its two-photon absorption cross-section in DMF at room temperature was measured to be 28.0×10^{-50} cm^4 s photon^{-1}. $[Pt(L^3)Cl]^+$ is able to selectively stain the cell nucleolus. This has been demonstrated by two-photon confocal imaging of live and methanol-fixed HeLa (human cervical carcinoma) and 3T3 (mouse skin fibroblasts) cells. This organelle specificity is likely to be related to its special affinity for proteins within cell nucleoli. As a result of such protein affinity, $[Pt(L^3)Cl]^+$ is an efficient RNA transcription inhibitor and shows rather profound cytotoxicity. On the other hand, the organelle-specific labelling and two-photon-induced luminescent properties of $[Pt(L^3)Cl]^+$ renders it a useful nuclear dye for the 3-dimensional reconstruction of optical sections of thick tissues, for example, mouse ileum tissues, by multiphoton confocal microscopy.

Keywords: imaging agents · optical tissue sectioning · organelle-specific labeling · platinum · two-photon imaging

Introduction

Owing to their outstanding photostability, decent quantum efficiency, long luminescent lifetime and good biocompatibility, coordination/organometallic complexes have attracted increasing attentions in biosensing and bioimaging.[1] For example, octahedral diimine complexes of Ru^{II}, Os^{II}, Re^{I} and Rh^{III} with the dipyrido[3,2-*a*:2′,3′-*c*]phenazine (dppz) ligand have been well known for their DNA intercalation capability.[2] An ethidium-conjugated Ru^{II} phenanthridine complex has recently been successfully developed for selective RNA sensing.[3] Cyclometalated Ir^{III} complexes with mixed phenylpyridine and diimine ligands have also been demonstrated to be versatile luminophores for biolabelling and bioimaging with tuneable luminescent colour.[1g,4] Recently, cyclometalated Pt^{II} complexes have been reported to be useful agents for protein staining and live cell imaging.[5]

In fact, attractive features of cyclometalated Pt^{II} systems for biolabelling and bioimaging go beyond their outstanding linear photophysical properties. A number of cyclometalated Pt^{II} systems have shown significant two-photon absorption cross-sections for two-photon-induced luminescence.[6–8] This makes them potentially useful in multiphoton microscopy, which has been regarded as the best non-invasive optical imaging technique for the study of cells, tissues and whole organisms.[9] At the moment, there are only a few commer-

[a] C.-K. Koo,[+] L. K.-Y. So,[+] Dr. K.-L. Wong, Y.-M. Ho, Dr. Y.-W. Lam, Dr. M. H.-W. Lam
Department of Chemistry and Biology
City University of Hong Kong
83 Tat Chee Avenue
Hong Kong SAR (China)
Fax: (+852) 2788-7406
E-mail: bhmhwlam@cityu.edu.hk
yunwlam@cityu.edu.hk

[b] Prof. Dr. K.-W. Cheah
Department of Chemistry, Hong Kong Baptist University
Waterloo Road, Kowloon Tong, Hong Kong SAR (China)

[c] C. C.-W. Cheng, Dr. W.-M. Kwok
Department of Applied Biology and Chemical Technology
Hong Kong Polytechnic University, Hung Hom
Kowloon (Hong Kong)

[+] These authors contributed equally to this work.

Supporting information for this article is available on the WWW under http://dx.doi.org/10.1002/chem.200902919.

cially available multiphoton fluorophores and most of them are organic-based dyes that generally produce short-lifetime fluorescence that are susceptible to interference by the auto-fluorescence of indigenous biomolecules in vitro and in vivo.[10] In this context, organometallic cycloplatinated systems are more advantageous because their much longer lifetime two-photon-induced ^{3}MLCT/^{3}IL (MLCT = metal–ligand charge transfer, IL = intraligand) phosphorescence can eliminate such interference through time-gated imaging techniques.[11] On the other hand, unlike the well-established, highly diversified, organic-based bioimaging probes with tailor-made specificity in intracellular localisation, literature on organelle-specific in vitro staining by organometallic-based multiphoton luminophores is scarce. It is envisioned that with proper functionalisation to bring about organelle- and functional-specific in vitro staining, cyclometalated Pt^{II} multiphoton luminophores can become very useful labelling, imaging and biosensing tools for molecular and cellular biological studies.

In our previous studies, we have developed a two-photon luminescent cyclometalated Pt^{II} system, $[Pt(L^1)X]$ (in which X = ancillary ligands such as Cl^- and PPh_3), based on a cyclometalating ligand, 2-phenyl-6-(1*H*-pyrazol-3-yl)pyridine (HL^1), containing a phenyl, a pyridyl and a pyrazolyl donor moiety.[12] The 1-pyrazolyl-*NH* moiety on the HL^1 constitutes a convenient site for easy functionalisation. Herein, we demonstrate a simple way to functionalise HL^1 though direct alkylation at 1-pyrazolyl-*NH* to conjugate a bioactive scaffold to the cycloplatinated luminophore so as to direct it to specific intracellular locations upon internalisation. We have chosen the triphenylphosphonium functionality to be the bioactive pendant because it is known to deliver different bioactive molecules to mitochondria both in vitro and in vivo.[13]

Results and Discussion

Design and synthesis: 6-Phenyl-2,2′-bipyridine (HC^N^N) and 1,3-di(pyridin-2-yl)benzene (HN^C^N) represent the basic designs of common π-conjugated tridentate cyclometalating ligands for cyclometalated Pt^{II} systems. However, these well-established ligand systems are difficult to be further modified or functionalised. The presence of a 1-pyrazolyl-*NH* on the new cyclometalating ligand, HL^1, enables its easy functionalisation by nucleophilic substitution.[14] We demonstrated this by direct alkylation of the 1-pyrazolyl-*NH* site on HL^1 with 1,5-dibromopentane to generate HL^2 in good yield. Further nucleophilic substitution of the terminal alkyl bromide on HL^2 by PPh_3 yielded the triphenylphosphonium-functionalised cyclometalating ligand, triphenyl{5-[3-(6-phenylpyridin-2-yl)-1*H*-pyrazol-1-yl]pentyl}phosphonium bromide (HL^3) (Scheme 1). The chloride salt of HL^3 was obtained by simple metathesis. The corresponding cyclometalated Pt^{II}–chloride complex, $[Pt(L^3)Cl]^+$, was obtained in good yield by direct metalation of HL^3 (chloride salt) with K_2PtCl_4 in glacial acetic acid. All of the new ligands and the cycloplatinated complex reported have been fully characterised by ^{1}H NMR spectroscopy and mass spectrometry.

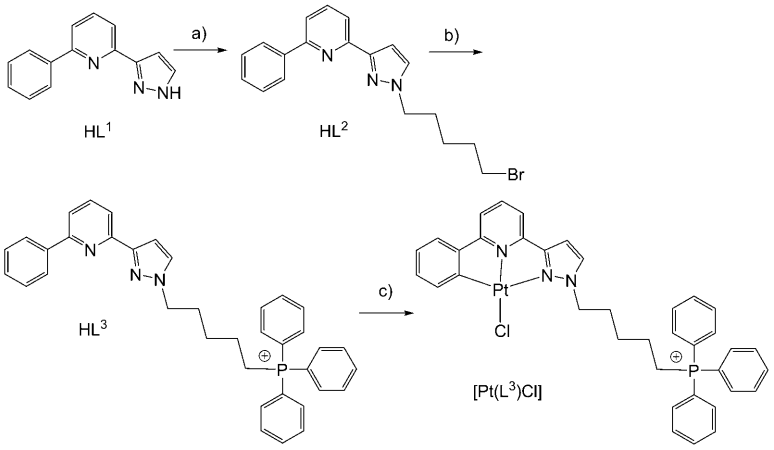

Scheme 1. Synthetic pathway for the preparation of HL^3 and the corresponding cyclometalated Pt^{II} complex $[Pt(L^3)Cl][PF_6]$: a) NaH, 1,5-dibromopentane; b) PPh_3; c) K_2PtCl_4, glacial acetic acid.

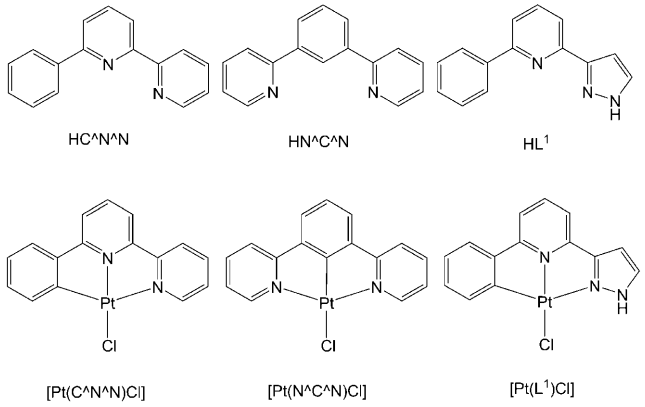

Linear photophysical studies: Electronic transition spectra of $[Pt(L^3)Cl]^+$ in various solvents are shown in Figure 1A. Spectroscopic properties of the complex show strong resemblances to its related $[Pt(L^1)Cl]$ complex. The UV-visible region is dominated by intense absorption bands at around

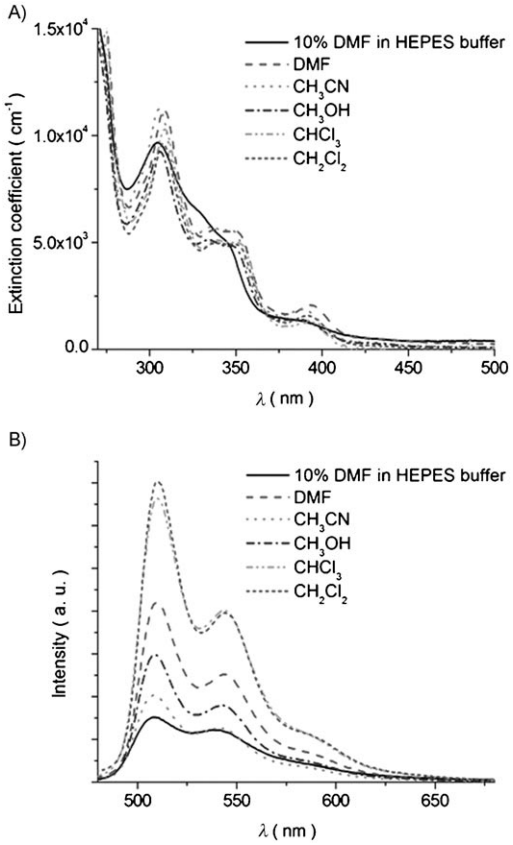

Figure 1. A) UV/Vis absorption and B) emission spectra of $[Pt(L^3)Cl]^+$ in various solvents (5×10^{-5} M) at 298 K.

275–375 nm with extinction coefficients (ε) in the order of 10^4 $dm^3 mol^{-1} cm^{-1}$ and a less intense band at around 380–410 nm with ε in the order of 10^3 $dm^3 mol^{-1} cm^{-1}$. With reference to previous spectroscopic studies of the analogous [Pt(C^N^N)Cl] and $[Pt(L^1)Cl]$ complexes, absorption bands at 275–375 nm are attributed to intraligand ($\pi(L)\rightarrow\pi^*(L)$) transitions, whereas the lower energy absorption band at 380–410 nm is assigned the spin-allowed $d\pi(Pt)\rightarrow\pi^*(L)$ metal-to-ligand charge-transfer (^{1}MLCT) transition. The λ_{max} of the lower energy band is solvent dependent and shifts from 387 nm in methanol to 393 nm in chloroform. This supports the assignment that the absorption band is from a charge-transfer transition.

$[Pt(L^3)Cl]^+$ exhibits strong luminescence in various aqueous/organic solvents under ambient conditions (see the Supporting Information). In acetonitrile at 298 K, $[Pt(L^3)Cl]^+$ gives a poorly resolved emission profile with λ_{max} at around 510 nm ($\tau=0.36$ μs; $\phi=0.10$) (Figure 1B). The large Stokes shift and the relatively long emission lifetime suggest that the emission is originated from a spin-forbidden triplet excited state. With reference to $[Pt(L^1)Cl]$, the emission peak of $[Pt(L^3)Cl]^+$ at around 510 nm is tentatively assigned as the ^{3}MLCT ($\pi^*(L)\rightarrow d\pi(Pt)$) transition, probably with some ^{3}IL ($\pi^*(L)\rightarrow\pi(L)$) character.[8] Compared with [Pt(C^N^N)Cl] the ^{3}MLCT emission of $[Pt(L^3)Cl]^+$ is blue-shifted (λ_{max} of the ^{3}MLCT emission of [Pt(C^N^N)Cl] in acetonitrile at 298 K is 550 nm). This is probably due to the more energetic $\pi^*(L)$ of the HL^3 cyclometalating ligand, which increases the ^{3}MLCT energy gap.

Two-photon properties: Upon two-photon excitation by a mode-locked femtosecond Ti:sapphire laser at 700 nm, a concentrated solution of $[Pt(L^3)Cl]^+$ in DMF (1×10^{-3} M) displayed an intense green emission at around 500 nm. The emission profile showed a strong resemblance to that obtained under linear one-photon excitation at 355 nm (see the Supporting Information). These similarities in both the profile and energy suggest that the emission is of the same origin as in single-photon excitation, that is, from a mixed ^{3}MLCT/^{3}IL excited state. As $[Pt(L^3)Cl]^+$ possessed no absorption band beyond 500 nm, the emission induced by 700 nm excitation was not likely to be due to any linear single-photon excitation process. A two-photon process was confirmed by a power-dependence experiment. From the log–log plot of the emission intensity against incident power, the linear regression with a slope of 1.98 indicates a two-photon excitation process (see the Supporting Information). The two-photon absorption cross-section of the complex was measured to be 28.0 GM (1 GM = 10^{-50} $cm^4 s\,photon^{-1}$) with Rhodamine 6G in DMF as the standard.[15] This is already much higher than the value of $\geq$0.1 GM suggested by Furuta et al. for optical imaging applications in live specimens.[16]

$[Pt(L^3)Cl]^+$-labelled nucleoli in fixed mammalian cells: Without the cationic triphenylphosphonium pendant, the cyclometalated Pt^{II} skeleton, that is, $[Pt(L^1)Cl]$, has already been found to be rapidly accumulated in live mammalian cells with even distribution in the cytoplasm but not in cell nuclei.[8] Cellular internalisation characteristics of $[Pt(L^3)Cl]^+$ and its affinity for cellular organelles was first tested on methanol-fixed mammalian cells, namely, human cervical carcinoma cells (HeLa) and normal mouse skin fibroblasts (3T3). Figure 2 shows the binding of $[Pt(L^3)Cl]^+$ to these fixed mammalian cells, HeLa (Figure 3A and B) and 3T3 (Figure 2C and D). Instead of selective staining of mitochondria, characteristic emission from $[Pt(L^3)Cl]^+$ (500–550 nm) was detected in both nuclei and cytoplasm with some nuclear domains strongly enriched (arrows) upon linear excitation at 405 nm. These heavily stained nuclear domains were also visible under differential interference contrast (DIC) microscopy (Figure 2B and D), suggesting they were nucleoli. To confirm the identity of these labelled structures, methanol-fixed HeLa cells were immunostained with an antibody against fibrillarin and then counterstained with $[Pt(L^3)Cl]^+$. Fibrillarin is a component of the snoRNPs and is commonly used as a nucleolar marker.[17] The $[Pt(L^3)Cl]^+$-stained nuclear domains (arrows, Figure 2E) completely co-localised with fibrillarin (Figure 2F), indicating those domains were nucleoli. Conversely, the immunofluorescence of FUS, a DNA and RNA binding protein known to be localised exclusively in the nucleoplasm,[18] did

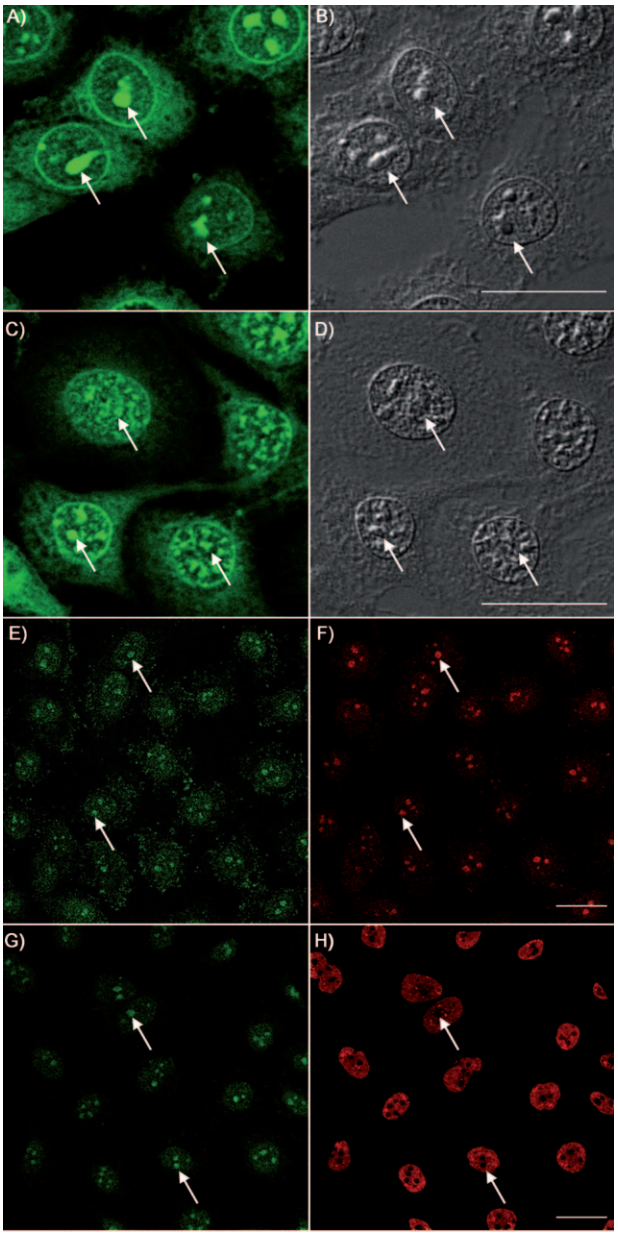

Figure 2. $[Pt(L^3)Cl]^+$-stained (1 mM) nucleoli in HeLa and 3T3 cells. $[Pt(L^3)Cl]^+$-labelled nuclear domains (arrows) in HeLa (A and B) and 3T3 (C and D) are shown. The labelled structures were visible under DIC microscopy (B and C). Staining with $[Pt(L^3)Cl]^+$ (E and G) (green) was co-localised with the immunofluorescence of fibrillarin (F, red) but did not colocalise with FUS (H, red), indicating that these domains were nucleoli (arrows). Scale bar = 25 μm.

not co-localised with $[Pt(L^3)Cl]^+$ staining (Figure 3G and H). $[Pt(L^3)Cl]^+$ can also label nucleoli when applied to live cells (see below). In summary, instead of binding mitochondria as in numerous other cellular imaging dyes that possess triphenylphosphonium pendants,[13] $[Pt(L^3)Cl]^+$ shows high affinity for the nucleolus of cultured mammalian cells.

$[Pt(L^3)Cl]^+$ is an effective multiphoton dye for cell nuclei: Given the high two-photon excitation cross-section of

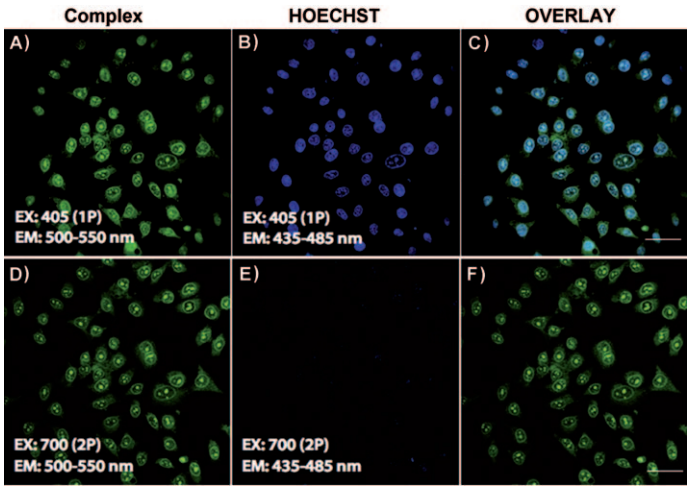

Figure 3. $[Pt(L^3)Cl]^+$ is an effective multiphoton dye for cell nuclei. The same group of HeLa cells co-stained with $[Pt(L^3)Cl]^+$ (1 mM) (green) and Hoechst 33342 (blue) were viewed with single-photon (A–C) and multiphoton (D–F) microscopy (EX = excitation, EM = emission, P = photon). Scale bars = 50 μm.

$[Pt(L^3)Cl]^+$ and its specific localisation properties in the nucleolus, we explored the application of $[Pt(L^3)Cl]^+$ as a nuclear dye for multiphoton confocal imaging. As shown in Figure 3, fixed HeLa cells were co-stained with $[Pt(L^3)Cl]^+$ and Hoechst 33342, a common DNA dye. The cells were imaged first by single photon excitation at 405 nm. Emission from the cycloplatinated complex was detected by a photomultiplier tube set to collect photons at 500–550 nm, whereas emission from Hoechst 33342 was detected by another photomultiplier tube set at 435–485 nm. The two detectors were adjusted in such a way that cross bleeding of light from each dye was minimised, as confirmed by the difference in intranuclear staining patterns of the two dyes (Figure 3A-C). Hoechst 33342-labelled heterochromatin in the nucleus, while $[Pt(L^3)Cl]^+$ labelled the nucleoli and, to lesser extent, the nuclear periphery and cytoplasm. The same group of cells were then imaged by a multiphoton excitation at 700 nm with the detection parameters unchanged. $[Pt(L^3)Cl]^+$ was strongly detectable by multiphoton imaging (Figure 3D), and the staining was clearly visible even when the power of the excitation laser was set to the minimum. Under these conditions, the fluorescence of Hoechst 33342 was too weak to be detected (Figure 3E). We therefore conclude that the high multiphoton cross-section of $[Pt(L^3)Cl]^+$ can be translated into its powerful performance as a cellular dye in multiphoton imaging.

One advantage of multiphoton microscopy is the capability of optical sectioning deep within thick tissues. To test this application of $[Pt(L^3)Cl]^+$, we incubated thick cryosections of various mouse tissues with the cyclometalated Pt^{II} complex, and imaged the staining under a multiphoton confocal microscope. As seen on single optical sections, cell nuclei of spleen (Figure 4A), ileum (Figure 4B), heart (Figure 4C) and kidney (Figure 4D) were labelled strongly with

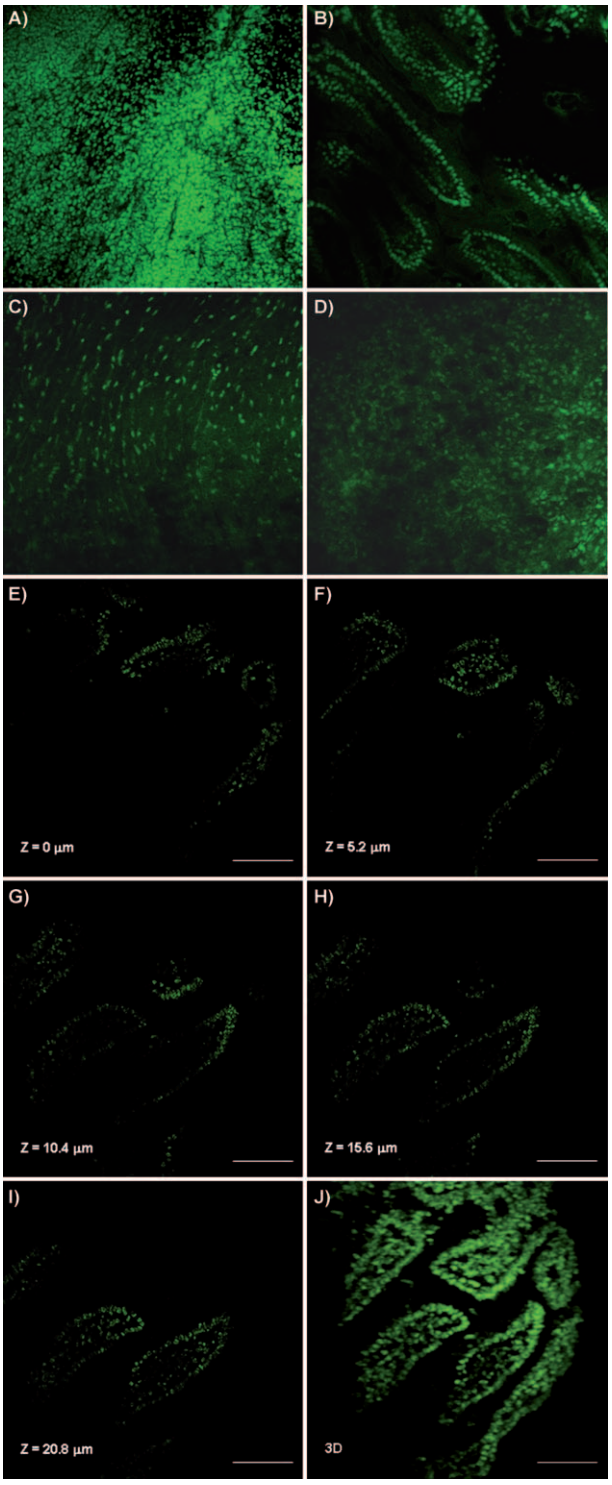

Figure 4. Multiphoton microscopy with $[Pt(L^3)Cl]^+$ as a nuclear dye. $[Pt(L^3)Cl]^+$ (1 mM) staining of various mouse tissues: spleen (A), ileum (B), heart (C) and kidney (D). E–I) Optical sections taken at different depths of a block of mouse ileum. J) 3D reconstruction of the optical sections. Scale bars = 75 μm.

$[Pt(L^3)Cl]^+$, with a weak cytoplasmic background. The prominent nucleolar staining observed in cultured cells was not evident in tissue sections. This may be due to the fact that nucleoli in primary tissues are smaller than those in tumour cells.[19] Figure 4 E–I shows optical sections taken at different depths of a block of mouse ileum, revealing the detailed structure of the small intestine, which can be rendered in a 3D reconstruction (Figure 4 J). Thus, our results demonstrates that $[Pt(L^3)Cl]^+$ can be used as a nuclear dye that is especially compatible with multiphoton confocal imaging.

Internalisation of $[Pt(L^3)Cl]^+$ by live cells and function as a transcription inhibitor: To investigate the effect of $[Pt(L^3)Cl]^+$ on living cells, we incubated HeLa cells with $[Pt(L^3)Cl]^+$ (1 mM). The cycloplatinated complex accumulated rapidly in living HeLa cells, with nucleoli clearly labelled within 15 min of incubation (Figure 5 A and B, arrows). The intracellular distribution of $[Pt(L^3)Cl]^+$ in live cells was essentially the same as that in fixed cells. However, these treated cells quickly rounded up and detached from the dish, suggesting that $[Pt(L^3)Cl]^+$ is quite toxic to cultured cells. To assess its cytotoxicity, we incubated HeLa and 3T3

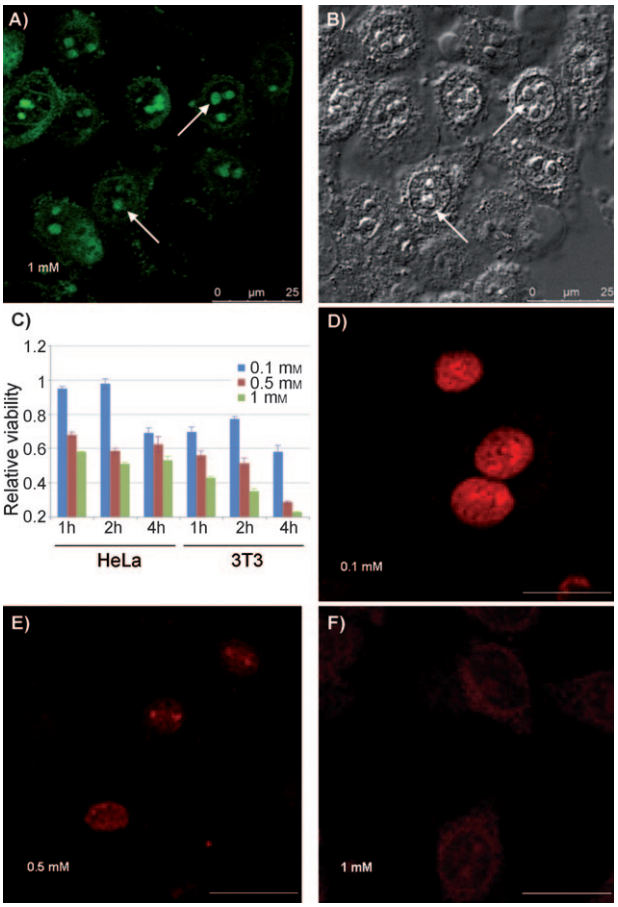

Figure 5. $[Pt(L^3)Cl]^+$ can be internalised by live cells and is a transcription inhibitor. A,B) HeLa cells imaged after incubation with $[Pt(L^3)Cl]^+$ (1 mM) in culture medium; arrows show the location of the nucleolus. C) Effect of $[Pt(L^3)Cl]^+$ on the viability of HeLa and 3T3 cells as determined by MTT assay (see Experimental Section). D–F) RNA synthesis in HeLa cells after treatment with $[Pt(L^3)Cl]^+$ at 0.1 (D), 0.5 (E) and 1 mM (F) for 15 min was determined by fluorouridine incorporation (red). Scale bars = 25 μm

cells with different concentrations of $[Pt(L^3)Cl]^+$ for 15 min, and rinsed the cells with fresh medium. Cell viability after this 15 min treatment was followed by MTT assay for up to 4 h. As shown in Figure 5C, significant cell death was observed 4 h after the 15 min exposure of cells to $[Pt(L^3)Cl]^+$ at concentration as low as 0.1 mM, and the extent and rapidity of cell death increased with increasing $[Pt(L^3)Cl]^+$ concentration. Interestingly, $[Pt(L^3)Cl]^+$ appeared to be more toxic to mouse 3T3 cells than to human HeLa cells (Figure 5C), suggesting that the toxicity of $[Pt(L^3)Cl]^+$ may depend on the species, cell types or transformation status of the cell lines.

Since the major target of $[Pt(L^3)Cl]^+$ is the nucleolus, which is a major site of RNA synthesis,[20] we tested the effect of $[Pt(L^3)Cl]^+$ on cellular transcription. Nascent RNA transcripts can be labelled by fluorouridine, which can be immunostained by an antibody against halogen-containing nucleosides.[21] In the absence of $[Pt(L^3)Cl]^+$, newly synthesised RNA, labelled by fluorouridine, was detected in a punctate pattern in cell nuclei (Figure 5D). After 15 min of incubation with $[Pt(L^3)Cl]^+$ at 0.1 mM, however, newly synthesised RNA was dramatically reduced in most cells (Figure 5E). At 0.5 mM, all RNA synthesis was abolished (Figure 5F). Hence, $[Pt(L^3)Cl]^+$ is a potent inhibitor of transcription.

The mechanism by which $[Pt(L^3)Cl]^+$ mediates its transcription inhibition is not clear. It is likely that on binding to endogenous structures in cells, the cyclometalated Pt^{II} complex blocks transcription-related reactions. It is therefore important to identify the biological molecules interacting with $[Pt(L^3)Cl]^+$. Since the majority of the cellular RNA accumulates in the nucleolus, it is possible that $[Pt(L^3)Cl]^+$ can bind to RNA. To test this hypothesis, we incubated methanol-fixed HeLa cells with RNase at a concentration that is sufficient for removing the cellular RNA content.[22] The RNase-treated cells were then stained with $[Pt(L^3)Cl]^+$. As shown in Figure 6A and B, RNase-digested cells (Figure 6B) were still labelled brightly by $[Pt(L^3)Cl]^+$, and the staining intensity and patterns were indistinguishable from those in untreated cells (Figure 6A). It is therefore unlikely that the interaction of $[Pt(L^3)Cl]^+$ with cellular structures is RNA dependent. To confirm this data, we incubated total cell lysate, purified DNA, RNA and proteins spotted on nitrocellulose membrane with $[Pt(L^3)Cl]^+$. As shown in Figure 6C, $[Pt(L^3)Cl]^+$ effectively stained total cell lysate on the blot, reproducing its cell binding properties observed by microscopy. Interestingly, $[Pt(L^3)Cl]^+$ did not bind to DNA or RNA but bound strongly to proteins, suggesting the staining of $[Pt(L^3)Cl]^+$ may be mediated by its specific interaction with some nuclear or nucleolar proteins.

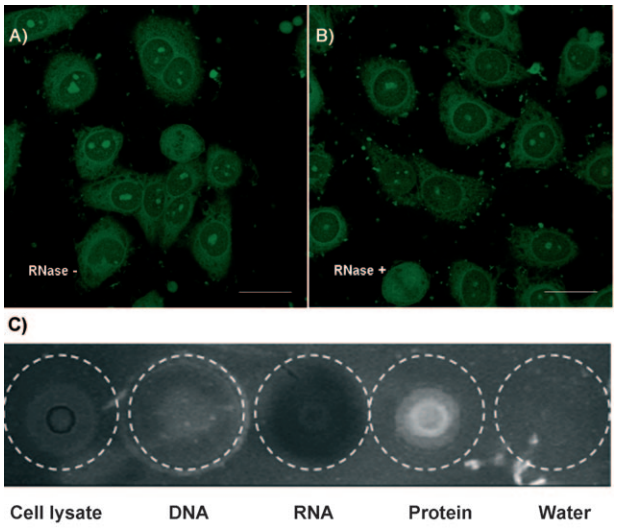

Figure 6. $[Pt(L^3)Cl]^+$ interacts with protein (A and B). The staining of $[Pt(L^3)Cl]^+$ (1 mM) (green) in HeLa cells with (B) or without (A) RNase digestion. Scale bars = 10 μm. C) A dot blot assay revealed that $[Pt(L^3)Cl]^+$ was bound to cell lysate and protein, but not to purified DNA or RNA.

Conclusion

We have developed an organometallic-based multiphoton molecular dye, $[Pt(L^3)Cl]^+$, with an outstanding affinity for cell nucleoli in both methanol-fixed and live mammalian cells. The dye is composed of a cyclometalated Pt^{II} luminophore and a cationic triphenylphosphonium pendant linked together by a C-5 methylene spacer. Binding of $[Pt(L^3)Cl]^+$ to cell nucleoli is likely to be brought about by the affinity of the complex for nuclear or nucleolar proteins within the organelle. The high two-photon absorption cross-section and luminescence quantum yield of $[Pt(L^3)Cl]^+$, together with its specific staining properties for cell nucleoli, makes it a powerful multiphoton imaging tool for optical sectioning of cells and thick tissues. Our work also demonstrates the versatility of the cyclometalated Pt^{II} luminophore with the phenyl-6-(1*H*-pyrazol-3-yl)pyridyl ligand as the basic building block for multiphoton biolabels and probes. Convenient functionalisation of the cyclometalating ligand with pendant moieties of different bioactivities and functionalities can be achieved with simple alkylation at the 1-pyrazolyl-*NH* site. Thus, with suitable functional pendants, a suite of biolabelling and biosensing probes for different sub-cellular targets can be generated from the multiphoton luminescent cyclometalated Pt^{II} building block.

Experimental Section

A human cervical carcinoma (HeLa) cell line and an adult male BALB/c mouse were used to perform part of the experiments in this work. According to the laws of Hong Kong Special Administrative Region (China), there is no need to obtain any licence for cell culture work. Regarding the BALB/c mouse, it was maintained and handled by procedures in compliance to the Prevention of Cruelty of Animals Ordinance (Cap. 169) of Hong Kong.

Materials and general procedures: All starting materials, 1,5-dibromopentane, PPh_3, NaH (60% by weight dispersed in mineral oil), KPF_6, NH_4PF_6 and K_2PtCl_4 were purchased from commercial sources and used

as received unless stated otherwise. Solvents used for synthesis were of analytical grade. THF was distilled from sodium/benzophenone prior to use. 2-Phenyl-6-(1*H*-pyrazol-3-yl)pyridine was prepared according to the published procedures.[12]

Compound HL^2: Freshly distilled THF (75 mL) was added to a mixture of 2-phenyl-6-(1*H*-pyrazol-3-yl)pyridine (1.12 g, 5 mmol) and NaH (60% by weight dispersed in mineral oil) (0.24 g, 6 mmol). The mixture was stirred for 15 min at room temperature. 1,5-Dibromopentane (2.31 g, 10 mmol) was then added and the mixture was heated to reflux for 24 h. After concentration under reduced pressure, the resulting crude solid was chromatographically purified by using 4:1 (v/v) petroleum ether/diethyl ether as the eluent to give a white crystalline solid (1.46 g, 78%). ^{1}H NMR (300 MHz, $CDCl_3$): δ = 8.09–8.14 (m, 2H; phenyl CH), 7.92 (dd, J = 0.9, 8.1 Hz, 1H; pyridyl CH), 7.78 (t, J = 7.8 Hz, 1H; pyridyl CH), 7.65 (dd, J = 0.9, 7.5 Hz, 1H; pyridyl CH), 7.38–7.52 (m, 4H; phenyl CH + pyrazolyl CH), 7.05 (d, J = 2.1 Hz, 1H; pyrazolyl CH), 4.20 (t, J = 6.9 Hz, 2H; aliphatic CH_2), 3.40 (t, J = 6.9 Hz, 2H; aliphatic CH_2), 1.85–2.02 (m, 4H; aliphatic CH_2), 1.44–1.56 (m, 2H; aliphatic CH_2); IR (KBr): $\tilde{\nu}$ = 3062, 1590 cm^{-1} (aromatic C=C); ESIMS: 371 $[M+1]^+$.

Compound HL^3: A mixture of 2-(1-(5-bromopentyl)-1H-pyrazol-3-yl)-6-phenylpyridine (1.11 g, 3 mmol) and PPh_3 (1.57 g, 6 mmol) in acetonitrile (50 mL) was heated to reflux with stirring for 72 h. After reaction, an aqueous solution (25 mL) of KCl (8.95 g, 120 mmol) was added. After concentration under reduced pressure, the resulting crude solid was chromatographically purified by using 2:1 (v/v) dichloromethane/methanol as the eluent to give a white solid (1.27 g, 72%). ^{1}H NMR (300 MHz, $CDCl_3$): δ = 8.06–8.12 (m, 2H; phenyl CH), 7.37–7.83 (m, 22H; phenyl CH + pyridyl CH + pyrazolyl CH), 6.87–6.89 (d, J = 6.9 Hz, 1H; pyrazolyl CH), 4.15 (t, J = 6.9 Hz, 2H; aliphatic CH_2), 3.00–3.11 (m, 2H; aliphatic CH_2), 1.87–2.00 (m, 2H; aliphatic CH_2), 1.56–1.67 (m, 2H; aliphatic CH_2), 1.48–1.57 (m, 2H; aliphatic CH_2); IR (KBr): $\tilde{\nu}$ = 3062, 1589 cm^{-1} (aromatic C=C); ESIMS: 553 $[M-Cl]^+$.

[Pt(L^3)Cl][PF$_6$]: A mixture of the free ligand HL^3 (0.35 g, 0.5 mmol) and K_2PtCl_4 (0.21 g, 0.5 mmol) in degassed glacial acetic acid (15 mL) was heated at reflux for 12 h to give a yellow solution. Addition of an aqueous solution (15 mL) of KPF_6 (0.92 g, 5 mmol) caused precipitation of a yellow solid. The precipitate was collected by filtration and washed with water and diethyl ether (0.38 g, 82%). ^{1}H NMR (300 MHz, $CDCl_3$): δ = 7.92–7.93 (d, J = 2.8 Hz, 1H; pyrazolyl CH), 7.83–7.90 (m, 5H; phenyl + pyridyl CH), 7.69–7.79 (m, 12H; phenyl CH), 7.45–7.47 (dd, J = 0.8, 8 Hz, 1H; pyridyl CH), 7.37–7.41 (m, 2H; phenyl + pyridyl CH), 7.25–7.29 (dt, J = 1.33, 7.47 Hz, 1H; phenyl CH), 7.15–7.19 (dt, J = 1.33, 7.47 Hz, 1H; phenyl CH), 6.78 (d, J = 2.8 Hz, 1H; pyrazolyl CH), 4.68 (t, J = 7.4 Hz, 2H; aliphatic CH_2), 3.25–3.33 (m, 2H; aliphatic CH_2), 2.13–2.15 (m, 2H; aliphatic CH_2), 1.81–1.80 (m, 4H; aliphatic CH_2); IR (KBr): $\tilde{\nu}$ = 3062, 1584 cm^{-1} (aromatic C=C); ESIMS: 782 $[M-PF_6]^+$.

Physical measurements and instrumentation: ^{1}H NMR spectra were recorded by using a Varian YH300 300 MHz NMR spectrometer. Electrospray (ESI) mass spectra were measured by using a PE SCIEX API 365 LC/MS/MS system. UV/Vis spectra were measured on a Hewlett Packard 8452A UV/Vis diode array spectrophotometer. Emission spectra were recorded by using a Horiba FluoroMax-3 spectrofluorimetric with a 5 nm slit width and 0.5 s integration time. Emission lifetime measurements were performed by using a SPEX FluoroLog 3-TCSPC spectrofluorimeter in the Fast MCS mode with a NanoLED N-370 as the laser source for excitation. Emission quantum yields were measured by the method of Demas and Crosby[23] with $[Ru(bpy)_3][(PF_6)_2]$ in degassed acetonitrile as the standard (ϕ_r = 0.062). Sample and standard solutions were degassed with at least three freeze–pump–thaw cycles.

Two-photon-induced emission measurements: The 700 nm pump source was from the fundamental of a femtosecond mode-locked Ti:sapphire laser system (output beam ≈150 fs duration and 1 kHz repetition rate). The laser was focused to a spot size of ≈50 μm through an f = 10 cm lens onto the sample. The emitting light was collected with a backscattering configuration into a 0.5 m spectrograph and detected by a liquid-nitrogen-cooled CCD detector. A power meter was used to monitor the uniform excitation.[24] To further confirm the two-photon process of the cyclometalated platinum(II) complex, the emission peak intensities were plotted as a function of the incident power at 700 nm.

Two-photon cross-section measurements: The theoretical framework and experimental protocol for the two-photon cross-section measurement have been outlined by Webb and Xu.[25] The two-photon excitation (TPE) ratios of the reference and sample systems were given by Equation (1):

$$\frac{\sigma_2^S \phi^S}{\sigma_2^R \phi^R} = \frac{C_R n_S F^S(\lambda)}{C_S n_R F^R(\lambda)} \quad (1)$$

in which ϕ is the quantum yield, C is the concentration, n the refractive index, and $F(\lambda)$ is the integrated photoluminescent spectrum. The superscripts S and R represent the sample and reference, respectively. In our measurements, we have ensured that the excitation flux and the excitation wavelengths are the same for both the sample and the reference. The two-photon absorption cross-section σ_2 of the cyclometalated platinum(II) complex $[Pt(L^3)Cl]^+$ was determined by using Rhodamine 6G as a reference.

Cell culture: HeLa and 3T3 cells were cultured in Dulbecco's Modified Eagle Medium (DMEM) from Gibco, supplemented with 10% foetal bovine serum (FBS) in the presence of antibiotic-antimycotic solution (Gibco). The cells were cultured in a humidified chamber with 5% CO_2 at 37 °C.

Immunofluorescence: For immunofluorescence experiments, HeLa cells were grown on 18 mm cover slips (no.1; Corning) and fixed with cold methanol for 10 min, washed three times with phosphate-buffered saline (PBS). Immunofluorescence staining was carried out as described previously.[26] Antibodies used were anti-fibrillarin polyclonal (dilution 1:100, Santa Cruz) and anti-FUS/TLS monoclonal (dilution 1:100, Santa Cruz), and TRITC conjugated secondary antibodies (Sigma). After immunofluoresence, cells were incubated with $[Pt(L^3)Cl]^+$ at 1 mM for 15 min. In some experiments, prior to mounting on slides, cover slips were incubated with 4 μM Hochest 33342 (Sigma) in water for 5 min to counterstain DNA. Coverslips were mounted in 50% glycerol and sealed with nail polish.

MTT cell viability assay: HeLa cells were plated in triplicates into 96-well tissue culture plates. After 24 h, cells were treated with $[Pt(L^3)Cl]^+$ at concentrations of 0, 0.1, 0.5 and 1 mM for 15 min. Cells were then washed with DMEM and replaced with new medium and incubated for 1, 2 and 4 h. The cells were then incubated with 0.5 mg mL^{-1} of 3-(4,5-dimethylthiazol-2-yl)-2,5-diphenyltetrazolium bromide (Sigma) for 30 min before being lysed with 1-isopropanol. Absorption was measured at 570 nm by using a microplate reader (PowerWave XS, BioTek). For comparison of cell viability between the treatments, a relative viability was calculated by dividing all the absorbance readings with those of cells not treated with $[Pt(L^3)Cl]^+$.

RNase treatment experiment: To investigate whether the cellular staining of $[Pt(L^3)Cl]^+$ was dependent on RNA integrity, HeLa cells were grown on cover slips, fixed with cold methanol for 10 min, were then washed thrice with PBS. The cells were treated with 100 mg mL^{-1} ribonuclease A from bovine pancreas (Sigma) for 30 min prior labelling with 1 mM of $[Pt(L^3)Cl]^+$ in PBS for 15 min. Cells were mounted in 50% glycerol and sealed with nail polish.

Histology: An adult (10 weeks old) male BALB/c mouse (obtained by the Lab Animal Unit, Chinese University of Hong Kong) was sacrificed by cervical dislocation. The mouse was maintained and handled by procedures in compliance to the Prevention of Cruelty of Animals Ordinance (Cap. 169) of Hong Kong. The heart, kidney, ileum and kidney were dissected and rinsed in PBS. The organs were snap-frozen in liquid nitrogen, embedded in tissue freezing medium (Jung) and sectioned on a cryostat (Jung CM 1500, Leica Instruments). The sections were dried on glass slides before being fixed in cold methanol (10 min, RT). After fixation, the sections were labelled with 1 mM of $[Pt(L^3)Cl]^+$ in PBS for 30 min. Hoechst 33342 (4 μM, 15 min) was used to counterstain DNA. Sections were mounted in 50% glycerol and sealed with nail polish.

Microscopy: For imaging $[Pt(L^3)Cl]^+$ entry into live HeLa cells, cells were grown on a glass-bottomed dish (MatTek) and CO_2-independent medium from Gibco were used, supplemented with 10% FBS. Cells were maintained at 37°C by use of the CO_2 microscope cage incubation system (Okolab).

For single-photon microscopy, images were collected by using a Leica TCS SPE spectral confocal microscope equipped with a diode laser (Leica). Specimens were imaged by using a 405 nm laser and through an ACS APO 40X NA 1.15 objective. A laser power of 20% was used in image acquisitions. For multiphoton microscopy, images were collected by using a Leica TCS SP5 spectral confocal microscope equipped with a Ti: sapphire laser (Leica). An emission of 700 nm and an HCX PL APO CS 40X NA 1.25 objective were used. A laser power of 1700 mW, a gain of 10% and an offset of 3% were used in image acquisitions. On both microscopes, $[Pt(L^3)Cl]^+$ emission was collected by a photomultiplier tube adjusted for wavelengths 500–550 nm and Hoechst 33342 emission was collected by PMT for 435–485 nm. For multiphoton imaging of thick mouse ileum tissue (Figure 5J), 95 optical sections (0.26 μm each) were recorded with LAS AF software (Leica).

Transcription assay: HeLa cells were treated with 0, 0.1, 0.5 and 1 mM of $[Pt(L^3)Cl]^+$ in DMEM for 15 min prior to being washed with new medium and fluorouridine was incorporated. Cells were incubated with 5′-fluorouridine (Sigma) at 1 mM in DMEM for 15 min. Cells were then fixed with cold methanol (10 min, RT) and immunostained with anti-BrdU monoclonal (dilution 1:100, Sigma) and TRITC conjugated secondary antibodies (Sigma) as previously described.[27] Cells were mounted in 50% glycerol and sealed with nail polish.

Dot blot assay: To investigate the interaction of $[Pt(L^3)Cl]^+$ with cellular structures, 2 μL of DNA, RNA and BSA at concentrations of 2 mg mL^{-1} and whole cell lysate at a protein concentration of 4 mg mL^{-1} were dotted on a nitrocellulose membrane (Whatman). DNA and RNA were extracted from HeLa cells by using TRIzol reagent (Invitrogen) and BSA (GE Healthcare) was dissolved in water to make the concentration. For whole cell lysate, HeLa cells were harvested by trysinisation (Invitrogen) and washed twice with PBS by centrifugation (2,000 rpm, 5 min, Kubota 2010 centrifuge). The cell pellet was then sonicated in water with an Ultrasonic processor (Cole Parmer) at an output power of 30 W of 10 s intervals until there was no visible cell debris. The dotted membrane was then soaked in 1 mM of $[Pt(L^3)Cl]^+$ in water for 5 min and rinsed three times to remove excess dye. A fluorometric image of the membrane was captured by using a Gel Doc (Bio Rad).

Acknowledgements

This work is funded by a GRF grant (CityU 101208) from the Hong Kong Research Grants Council. K.-L.W. acknowledges the Research Scholarship Enhancement Scheme from City University of Hong Kong.

[1] a) W. M. Leevy, J. R. Johnson, C. Lakshmi, J. D. Morris, M. Marquez, B. D. Smith, *Chem. Commun.* **2006**, 1595–1597; b) A. Nonat, C. Gateau, P. H. Fries, M. Mazzanti, *Chem. Eur. J.* **2006**, *12*, 7133–7150; c) J. H. Yu, D. Parker, R. Pal, R. A. Poole, M. J. Cann, *J. Am. Chem. Soc.* **2006**, *128*, 2294–2299; d) K. K. W. Lo, K. H. K. Tsang, K. S. Sze, C. K. Chung, T. K. M. Lee, K. Y. Zhang, W. K. Hui, C. K. Li, J. S. Y. Lau, D. C. M. Ng, N. Zhu, *Coord. Chem. Rev.* **2007**, *251*, 2292–2310; e) A. S. Chauvin, S. Comby, B. Song, C. D. B. Vandevyver, J. C. G. Bünzli, *Chem. Eur. J.* **2008**, *14*, 1726–1739; f) R. Pal, D. Parker, *Org. Biomol. Chem.* **2008**, *6*, 1020–1033; g) K. K. W. Lo, K. Y. Zhang, S. K. Leung, M. C. Tang, *Angew. Chem.* **2008**, *120*, 2245–2248; *Angew. Chem. Int. Ed.* **2008**, *47*, 2213–2216; h) J. A. G. Williams, *Chem. Soc. Rev.* **2009**, *38*, 1783–1801.

[2] a) K. E. Erkkila, D. T. Odom, J. K. Barton, *Chem. Rev.* **1999**, *99*, 2777–2795, and the references therein; b) C. A. Puckett, J. K. Barton, *J. Am. Chem. Soc.* **2007**, *129*, 46–47; C. A. Puckett, J. K. Barton, *J. Am. Chem. Soc.* **2009**, *131*, 8738–8739.

[3] N. A. O'Connor, N, Stevens, D. Samaroo, M. R. Solomon, A. A. Marti, J. Dyer, H. Vishwasrao, D. L. Akins, E. R. Kandel, N. J. Turro, *Chem. Commun.* **2009**, 2640–2642.

[4] a) M. Yu, Q. Zhao, L. Shi, F. Li, Z. Zhou, H. Yang, T. Yi, C. Huang, *Chem. Commun.* **2008**, 2115–2117; b) K. K. W. Lo, P. K. Lee, J. S. Y. Lau, *Organometallics* **2008**, *27*, 2998–3006; c) K. K. W. Lo, K. Y. Zhang, S. K. Leung, M. C. Tang, *Angew. Chem.* **2008**, *120*, 2245–2248; *Angew. Chem. Int. Ed.* **2008**, *47*, 2213–2216; d) J. S. Y. Lau, P. K. Lee, K. H. K. Tsang, C. H. C. Ng, Y. W. Lam, S. H. Cheng, K. K. W. Lo, *Inorg. Chem.* **2009**, *48*, 709–718; e) K. Y. Zhang, K. K. W. Lo, *Inorg. Chem.* **2009**, *48*, 6011–6025.

[5] P. Wu, E. L.-M. Wong, D.-L. Ma, G. S.-M. Tong, K.-M. Ng, C.-M. Che, *Chem. Eur. J.* **2009**, *15*, 3652–3656.

[6] a) S. K. Hurst, M. G. Humphrey, T. Isoshima, K. Wostyn, I. Asselberghs, K. Clays, A. Persoons, M. Samoc, B. Luther-Davices, *Organometallics* **2002**, *21*, 2024–2026; b) S. Das, A. Nag, D. Goswami, P. K. Bharadwaj, *J. Am. Chem. Soc.* **2006**, *128*, 402–403; c) J. L. Humphrey, D. Kuciauskas, *J. Am. Chem. Soc.* **2006**, *128*, 3902–3903; d) E. Glimsdal, M. Carlsson, B. Eliasson, B. Minaev, M. Lindgren, *J. Phys. Chem. A* **2007**, *111*, 244–250; e) X. B. Zhang, J. K. Feng, A. M. Ren, *J. Phys. Chem. A* **2007**, *111*, 1328–1338.

[7] S. W. Botchway, M. Charnley, J. W. Haycock, A. W. Parker, D. L. Rochester, J. A. Weinstein, J. A. Gareth Williams, *Proc. Natl. Acad. Sci. USA* **2008**, *105*, 16071–16076.

[8] C.-K. Koo, K.-L. Wong, C. W.-Y. Man, Y.-W. Lam, L. K.-Y. So, H.-L. Tam, S.-W. Tsao, Cheah, K.-W. Cheah, K.-C. Lau, Y.-Y. Yang, J.-C. Chen, M. H.-W. Lam, *Inorg. Chem.* **2009**, *48*, 872.

[9] a) W. R. Zipfel, R. M. Williams, W. W. Web, *Nat. Biotechnol.* **2003**, *21*, 1369–1377; b) F. Helmchen, W. Denk, *Nat. Methods* **2005**, *2*, 932–940.

[10] a) For example, see: http://www.drbio.cornell.edu/cross_sections.html; b) M. A. Albota, C. Xu, W. W. Webb, *Appl. Opt.* **1998**, *37*, 7352–7356; c) C. Xu in *Confocal and Two-Photon Microscopy* (Ed.: A. Diaspro), Wiley, New York, **2002**.

[11] a) D. Parker, *Coord. Chem. Rev.* **2000**, *205*, 109–130; b) S. Phimphivong, S. S. Saavedra, *Bioconjugate Chem.* **1998**, *9*, 350–357.

[12] C.-K. Koo, Y.-M. Ho, C.-F. Chow, M. H.-W. Lam, W.-Y. Wong, *Inorg. Chem.* **2007**, *46*, 3603–3612.

[13] a) R. A. J. Smith, C. M. Porteous, A. M. Gane, M. P. Murphy, *Proc. Natl. Acad. Sci. USA* **2003**, *100*, 5407–5412; b) K. M. Robinson, M. S. Janes, M. Pehar, J. S. Monette, M. F. Ross, T. M. Hagen, M. P. Murphy, J. S. Beckman, *Proc. Natl. Acad. Sci. USA* **2006**, *103*, 15038–15043; c) M. P. Murphy, R. A. Smith, *Annu. Rev. Pharmacol. Toxicol.* **2007**, *47*, 629–656; d) L. Biasutto, A. Mattarei, E. Marotta, A. Bradaschia, N. Sassi, S. Garbisa, M. Zoratti, C. Paradisi, *Bioorg. Med. Chem. Lett.* **2008**, *18*, 5594–5597; e) S. Liu, Y.-S. Kim, S. Zhai, G. Hou, *Bioconjugate Chem.* **2009**, *20*, 790–798.

[14] a) S. Trofimenko, *J. Am. Chem. Soc.* **1970**, *92*, 5118; b) K. L. Mann, J. C. Jeffery, J. A. McCleverty, P. Thornton, M .D. Ward, *J. Chem. Soc. Dalton Trans.* **1998**, 89–98; c) K. L. V. Mann, J. C. Jeffery, J. A. McCleverty, M. D. Ward, *J. Chem. Soc. Dalton Trans.* **1998**, 3029–3036.

[15] a) M. Albota, D. Beljonne, J. L. Bredas, J. E. Ehrlich, J. Y. Fu, A. A. Heikal, S. E. Hess, T. Kogej, M. D. Levin, S. R. Marder, D. McCord-Maughon, J. W. Perry, H. Rockel, M. Rumi, C. Subramaniam, W. W. Webb, X. L. Wu, C. Xu, *Science* **1998**, *281*, 1653–1657; b) T. Kohl, K. G. Heinze, R. Kuhlemann, A. Koltermann, P. Schwille, *Proc. Natl. Acad. Sci. USA* **2002**, *99*, 12161.

[16] T. Furuta, S. S.-H. Wang, J. L. Dantzker, T. M. Dore, W. J. Bybee, E. M. Callaway, W. Denk, R. Y. Tsien, *Proc. Nat. Acad. Sci. USA* **1999**, *96*, 1193–1200.

[17] S. L. Reichow, T. Hamma, A. R. Ferré-D'Amaré, G. Varani, *Nucleic Acids Res.* **2007**, *35*, 1452–1464.

[18] M. Gardiner, R. Toth, F. Vandermoere, N. A. Morrice, J. Rouse, *Biochem. J.* **2008**, *415*, 297–307.

[19] D. Treré, C. Ceccarelli, L. Montanaro, E. Tosti, M. Derenzini, *J. Histochem. Cytochem.* **2004**, *52*, 1601–1607.

[20] Y. W. Lam, L. Trinkle-Mulcahy, A. I. Lamond, *J. Cell Sci.* **2005**, *118*, 1335–1337.

[21] F. M. Boisvert, M. J. Kruhlak, A. K. Box, M. J. Hendzel, D. P. Bazett-Jones, *J. Cell Biol.* **2001**, *152*, 1099 – 1106.
[22] A. Krishan, *J. Cell Biol.* **1975**, *66*, 188 – 193.
[23] J. N. Demas, G. A. Crosby, *J. Phys. Chem.* **1971**, *75*, 991 – 1024.
[24] S. Tanabe, K. Tamai, K. Hirao, N. Soga, *Phys. Rev. B* **1993**, *47*, 2507 – 2514.
[25] C. Xu, W. W. Webb, *J. Opt. Soc. Am. B* **1996**, *13*, 481 – 491.
[26] Y. W. Lam, C. E. Lyon, A. I. Lamond, *Mol. Biol. Cell* **2002**, *13*, 2461 – 2473.
[27] F. M. Boisvert, M. J. Kruhlak, A. K. Box, M. J. Hendzel, D. P. Bazett-Jones, *J. Cell Biol.* **2001**, *152*, 1099 – 1106.

Received: October 22, 2009
Published online: March 22, 2010

